THE LAGGED CELL-TRANSMISSION MODEL

Carlos F. Daganzo, Inst. of Transp. Studies, Univ of California, Berkeley, California, USA

ABSTRACT

Cell-transmission models of highway traffic are discrete versions of the simple continuum (kinematic wave) model of traffic flow that are convenient for computer implementation. They are in the Godunov family of finite difference approximation methods for partial differential equations. In a cell-transmission scheme one partitions a highway into small sections (cells) and keeps track of the cell contents (number of vehicles) as time passes. The record is updated at closely spaced instants (clock ticks) by calculating the number of vehicles that cross the boundary separating each pair of adjoining cells during the corresponding clock interval. This average flow is the result of a comparison between the maximum number of vehicles that can be "sent" by the cell directly upstream of the boundary and those that can be "received" by the downstream cell.

The sending (receiving) flow is a simple function of the current traffic density in the upstream (downstream) cell. The particular form of the sending and receiving functions depends on the shape of the highway's flow-density relation, the proximity of junctions and on whether the highway has special (e.g., turning) lanes for certain (e.g., exiting) vehicles. Although the discrete and continuum models are equivalent in the limit of vanishingly small cells and clock ticks, the need for practically sized cells and clock intervals generates numerical errors in actual applications.

This paper shows that the accuracy of the cell-transmission approach is enhanced if the downstream density that is used to calculate the receiving flow(s) is read ℓ clock intervals earlier than the current time, where ℓ is a non-negative integer that should be carefully chosen. The rationale for the introduction of this lag is explained in the paper. The lagged cell-transmission model is related (but not equivalent) to both Godunov's first order method for general flow-density relations and Newell's exact method for concave flow density relations. It is easier to apply and more general than the latter, and more accurate than the former. In fact, if the flow-density relation is triangular and the lag is chosen optimally, then the lagged cell-tansmission model is a conservative, second order, finite difference scheme. As a result, very accurate results can be obtained with relatively large cells. Accuracy formulae and sample illustrations are presented for both the triangular and the general case.

1. INTRODUCTION

This paper describes a new finite difference approximation for the kinematic wave model of traffic flow formulated by Lighthill and Whitham (1955) and Richards (1956), called here the LWR model, and for the generalized continuum model that applies to freeways with special lanes (Daganzo, 1995). The proposed scheme is conservative, in that vehicles are not created or lost during the simulation except at the highway's entrances and exits, like the procedures described in Bui et al (1992), Lebacque (1993) and Daganzo (1993 and 1993a). Unlike its predecessors, however, the proposed scheme is not in Godunov's family of finite difference approximations (see Godunov, 1961, or LeVeque, 1992), and is more accurate than they are.

In the new scheme, flows across the boundary between two cells are calculated with a sending/receiving metaphor similar to that introduced in Lebacque (1993) and Daganzo (1993a), using only information from the two neighboring cells.[1] Such a metaphor is called here the cell-transmission (CT) model. The CT recipe has been modified to model junctions (Daganzo, 1994) and highway links with special lanes, e.g., for turning or high occupancy vehicles (Daganzo, Lin and DelCastillo, 1995). These modifications make it possible to model complex networks. The similarity between the new and the old CT recipes ensures that these modifications can be extended trivially to the new method. Thus, the improvement in accuracy obtained with the new method should apply to network models.

The main difference between the new approach and the original CT recipe is that the density of the downstream cell, used to calculate the "receiving" flow, is now taken from an earlier time, with a lag of ℓ simulation clock intervals. Newell's exact solution method for concave flow-density relations (Newell, 1993) is also based on the introduction of lags. Lags are useful for highway traffic modeling because traffic information travels several times more slowly in the upstream than in the downstream direction. In our case, we shall see that if the two wave speeds (forward and backward) are independent of density, then the lagged cell-transmission (LCT) model turns out to be second order accurate.

Because this paper is closely related to Daganzo (1993a), the reader is referred to that reference for more extensive introductory remarks. The remainder of this paper is organized as

---

[1] Lebacque (1993) uses the terms "local demand" and "local supply" to express the metaphor.

follows. Section 2 presents experimental evidence pertaining to wave speeds and illustrates by means of an example the minor difficulties one encounters with the LWR theory when the wave speed does not decline with density monotonically, i.e., when the flow-density relation is non-concave; in particular, it is shown that the "stable" LWR solution can have waves emanating from a shock. The new finite difference approximation is then presented in Section 3, together with an analysis of its accuracy and stability. The paper concludes with some examples (Sec. 4) that illustrate the results of Sec. 3.

2. NON-DECLINING WAVE SPEEDS

The LWR model is intended to describe traffic on large scales of observation, where it makes sense to define a density function $k(t, x)$ and a flow function $q(t, x)$ in time-space (t, x). It is based on the assumption that q and k are locally related by a flow-density relation $q = T(k, t, x)$. When the highway is homogeneous and its features do not depend on time (e.g. no incidents or moving bottlenecks) then the relation only includes k as an argument:

$$q = T(k). \tag{1}$$

This is the case that will receive attention for the most part of this paper.

Flow and density are also related by the conservation equation:

$$k_t + q_x = 0, \tag{2}$$

where subscripts have been used to denote partial derivatives.[2] Thus, it is possible to eliminate q from (1) and (2). The result is the following simple first order quasi-linear partial differential equation in k:

$$k_t + T_k k_x = 0. \tag{3}$$

In this equation k_t and k_x are functions of t and x, and T_k is a known function of k. This is the conventional way of expressing the LWR model for numerical approximations.

If T_k is independent of k then the solution to (3) has the form: $k(t, x) = g(x-T_k t)$; i.e., it is a translationally symmetric function (wave) with wave velocity T_k . The particular form of g depends on the boundary conditions. For example, for the initial value problem where $k(0, x)$ is given, $g(x) = k(0, x)$ and

---

[2]Subscripts t, x and k will be used in this paper to denote partial derivatives of the subscripted variable with respect to time, distance and density. All other subscripts, e.g., i, j, and ℓ, will be indices for the subscripted variables.

$$k(t, x) = k(0, x\text{-}T_k t). \tag{4}$$

The wave velocity T_k also plays an important role in the quasi-linear case. In this case too, the density is constant along wave-lines (characteristics) issued from the boundary, but the wave-lines can now focus and cross. The solution can be extended into these regions of the (t, x) plane by introducing curves, called shocks in the LWR theory, where k(t, x) is discontinuous. Conservation of vehicles across such discontinuities results in the following equation for the shock velocity, u :

$$u = \Delta q / \Delta k \tag{5}$$

where Δq and Δk represent the changes in flow and density across the shock.

Equations (3) and (5), however, are not always enough to specify a solution. It turns out that shocks can often be introduced in more than one way to form a mathematically correct solution of a properly formulated problem; i.e., a solution that is consistent with (3) and (5) and with the initial data. If the problem has been properly formulated, however, i.e., if it makes physical sense, then there should be one and only one solution that makes physical sense. This solution can be identified with a standard stability argument; i.e., by making sure that the solution does not come undone if a small perturbation is introduced in it.[3]

If $q = T(k)$ is represented by a curve as in the top part of Fig. 1, then the wave velocity is the slope of the curve. Note that if the curve is concave, then the wave velocity declines with density, and also with the traffic speed. That is, waves focus (into a shock) when traffic decelerates and fan out (as an expanding wave) when it accelerates. The best evidence available and common sense indicates that the maximum wave speed in the forward direction, obtained for low densities, is comparable with the free-flow traffic speed, e.g., on the order of 60 mi/hr (27 m/s), and that the backward wave speeds are several times slower. This is illustrated on the bottom part of Fig. 1, which has been taken from Cassidy (1998).

Additional experiments correlating data from several detectors point to the existence of expansive deceleration waves and focused acceleration waves in congested traffic (Windover and Cassidy, 1997). Related anecdotal evidence has also been recorded by this author on Highway US-50 West of Placerville, California. This is a heavily traveled two-lane highway with very few intersections, which experienced a sustained capacity-reducing incident on the particular date. This created queues of many miles on both sides of the road. On crossing the incident location and traveling past the queue in the opposite direction, this author noted a period of a minute or two (spanning between 1 and 2 highway miles) where rather dense traffic appeared to be coasting toward the end of the queue(!). This was not a stop-and-go wave, for those were observed within

[3] The physically relevant solution must be one where the shocks are "stable"; i.e., where if (at any given time, t_o) one were to replace a shock by a quick but gradual transition in density between the values prevailing on both sides of the shock, then the shock would reform itself and the solution would quickly approach the original (for $t > t_o$).

the queue and they had a much shorter period (from the stand point of the moving observer).

This coasting effect cannot be explained by the LWR theory with a concave T(k), since in that theory the end of a queue should involve a transition with just a few vehicles. It cannot be explained either by linear car-following models (e.g., as in Herman et al, 1959), but it can be explained by the LWR theory with a non-concave T(k) and a "tail" to the right (such as that in the top part of Fig. 1) and/or by the corresponding non-linear car-following model. We do not wish to speculate further about this phenomenon in this paper, since the goal of this comment is only to establish the desirability of having numerical methods that can treat non-concave T(k) relations. Such methods can be used for prediction if such tail exists, or they may help disprove its existence if it does not.

Improved numerical methods are desirable because the exact procedures in Newell (1993) cannot be used with non-concave relations, and because the cell-transmission approaches introduce some error into the calculation. Before the new method is presented, a brief example is introduced which illustrates the stability condition for non-concave T(k).

2.1 An example

Let us examine how a line of cars comes to a halt according to the LWR theory, when the flow-density relation, T(k), is as in Fig. 2a. We assume that the corners of our curve have been smoothed very slightly, not enough to be seen in the figure, so that the wave velocity is defined for all densities.[4]

It is assumed that the leading cars in the line are in state A' (q = 0.6 veh/sec, k = 12 veh/Km) and that heavier traffic (state A with q = 1 veh/sec and k = 20 veh/Km) is found 6 Km upstream of the leading car; see Fig. 2b. The origin of the (t, x) coordinates has been chosen so that the first car stops at x = 0 (Km) when t = 0 (secs).

Part b of the figure satisfies (3) and (5) but is unstable. To see this, note that if the shock at time t_o is replaced by a smooth transition in density (e.g., at t_o = 400s) then a fan of waves would emanate from it and the solution would not evolve into the future ($t > t_o$) as originally assumed because the fan would introduce a state "E" into the solution.

Part c is the stable solution to this problem. It includes a fan of waves (carrying state "E") that are issued tangentially from the shock at the point where it bends. That this solution is stable is seen by noting that if the shock is replaced by a smooth but rapid transition in density anywhere, even at the point where the shock bends, then the wave pattern so generated will match the one in the solution.[5] This means that no new states can be introduced into the solution of Fig. 2c by an

---

[4]Smoothed piece-wise linear q-k curves such as ours, are good for illustration purposes because they lead to solutions that are simple and easy to interpret.

[5]To check stability at the point where the shock bends, one should treat the transition from A' to A as being rapid but smooth, remembering that the diagram of Fig. 2c is on a large scale. On a resolution scale where the transition from A' to A can be discerned the stable shock would have to bend gradually. Furthermore, waves would peel off from it as it curves. This detailed geometry is consistent with the macroscopic picture painted in Fig. 2c.

infinitesimal perturbation and that the solution is the one that would arise physically.

That Fig. 2.c is the relevant solution can also be verified from microscopic (car-following) considerations, although this is more tedious. This statement is based on the principle that *any* asymptotically stable car-following model, in the sense of Herman et al (1959), must be consistent with the corresponding (stable) LWR result; e.g. with the macroscopic result of Fig. 2c in our case, provided of course that the equilibrium speed-spacing relation is consistent with the T(k) of Fig. 2a and that the initial conditions are also consistent with those of Fig. 2. The development of a coasting state, such as state "E" of Fig. 2c, is demonstrated with car-following theory in a longer version of this paper (Daganzo, 1997). Figure 10 of that reference shows that the car-following vehicle trajectories indeed develop a coasting state when a platoon is brought to a halt.

3. THE LAGGED CELL-TRANSMISSION RULE

3.1 Background

The cell-transmission model can be applied to unimodal T(k) curves with maximum flow q_{max}. First one defines two monotonic curves that take values in the interval $[0, q_{max}]$, as shown in Fig. 3: a non-increasing *receiving* curve R(k) and a non-decreasing *sending* curve S(k). The symbol k^o is used to denote one of the densities where the maximum is achieved.

A rectangular lattice with spacings ϵ and d is then overlaid on the (t, x)-plane, as shown on Fig. 4. It is understood that traffic flows in the direction of increasing x. The x-coordinates of the lattice points, denoted $\{x_j\}$, represent the center of the "cells" into which the highway has been discretized, and the t-coordinates $\{t_i\}$, the times at which the cell densities are evaluated. The numbering scheme is such that $x_{j+1} > x_j$ and $t_{i+1} > t_i$ so that traffic advances in the direction of increasing j .

If we now let $K(t_i, x_j)$ denote the average density estimated for cell j at time t_i, and we write $Q(t_i + \epsilon/2, x_j + d/2)$ for the average flow that would advance from cell j to cell j+1 (i.e., crossing location $x_j + d/2$) in the time interval $[t_i , t_i{+}1]$, then we require:

$$K(t+\epsilon, x) = K(t, x) - (\epsilon/d)[\, Q(t+\epsilon/2, x+d/2) - Q(t+\epsilon/2, x-d/2)] \qquad (6)$$

by virtue of conservation. The subscripts i and j have been omitted in (6) for simplicity of notation. This will be done from now on when reference to particular cells and/or a time slices is not necessary. In these cases it should be understood that (t, x) is a point on the lattice.

The cell transmission model is completed by a formula that gives Q in terms of the sending and receiving functions evaluated at the upstream and downstream cells,

$$Q(t+\epsilon/2, x+d/2) = \min\{\, S(K(t, x)) , R(K(t, x+d)) \,\}, \qquad (7)$$

and by specifying that

$$\epsilon \leq d/|T_k|_{max} , \tag{8}$$

where $|T_k|_{max}$ is the maximum of the absolute wave speed for the given T(k) relation. For maximum accuracy, one should choose

$$\epsilon = d/|T_k|_{max} . \tag{9}$$

Equation (8) ensures that data from outside the two neighboring cells cannot influence the calculated flow, which is a requirement for convergence.

Recall now that in Godunov's approach, Eq.(7) would be the flow at the discontinuity in the *stable* solution of a Riemann problem[6] for which the upstream density, k^u , is that of the upstream cell, $k^u = K(t, x)$, and the downstream density, k^d , is that of the downstream cell, $k^d = K(t, x+d)$; see LeVeque, 1992. The reader can verify, e.g., using the ideas in Sec. 2, that Eq. (7) indeed yields the stable flow at the location of the discontinuity for a Riemann problem with densities K(t, x) and K(t, x+d) -- no matter how these two values are chosen -- if the T(k) relation is unimodal. This establishes that the CT model (6-7) is in Godunov's family of finite difference approximations for unimodal T(k)'s.

3.2 The new rule.

Let $S_{k,\, max}$ and $|R_k|_{max}$ denote the maximum (absolute) wave speeds in the forward and reverse directions, and $|T_k|_{max}$ the maximum in any direction. We show below that whenever $|R_k|_{max} << S_{k,max} = |T_k|_{max}$, as one would expect for most traffic streams, it is advantageous to read the sending and receiving flows from different time slices. That is, one can define a lag, $\ell = 0, 1, 2, ...$, and use:

$$Q(t+\epsilon/2, x+d/2) = \min\{ S(K(t, x)) , R(K(t-\ell\epsilon, x+d)) \}, \tag{10}$$

instead of (7). This corresponds to the stencil depicted in Fig. 4, which predicts the flow at point "P" when $\ell = 2$. The special case with $\ell = 0$ reduces to the conventional cell-transmission rule.

It turns out (somewhat intuitively perhaps) that rule (10) is most accurate when the velocity of the wave reaching "P" happens to match the slope of one of the arrows in the figure; i.e., if the prediction at "P" is evaluated as close as possible to the source of its wave. This will be the basis for our choice for ℓ. It also turns out, for stability reasons, that the backward slope of the arrow in

[6]A Riemann problem is an initial value problem where the initial density is a step function with one step; i.e., $k(0, x) = k^d$ if $x > x^o$, and $k(0, x) = k^u$ if $x \leq x^o$.

our diagram should not be less than the maximum backward wave speed, $|R_k|_{max}$. This means that ℓ must satisfy:

$$\epsilon \;\leq\; d \,/\, [|R_k|_{max}\,(2\ell+1)]. \tag{11}$$

A choice of ℓ where (11) is as close as possible to a pure equality is recommended; i.e., where:

$$\ell \;\approx\; \tfrac{1}{2}\,[d(\epsilon|R_k|_{max})^{-1} - 1]. \tag{12}$$

The accuracy of (8), (10) and (12) is evaluated below. The steps parallel those in Sec. 4 of Daganzo (1993a).

3.3 Error estimation.

Consider a region of the time-space plane where the waves move back (congested traffic). Then, (6) and (10) may be rewritten as:

$$K(t+\epsilon, x) = K(t, x) - (\epsilon/d)[\, T(K(t-\ell\epsilon, x+d) - T(K(t-\ell\epsilon, x)\,] \tag{13}$$

since in this region T(k) = R(k).

In the exact theory, the solution at time t+ϵ is related to the solution at time t by:

$$k(t+\epsilon, x) = k(t, x-T_k\epsilon)$$

where T_k is evaluated for the density prevailing at $(t, x-T_k\epsilon)$. Thus, in a region where $K > k^o$, it is convenient to rewrite (13) in the following manner:

$$K(t+\epsilon, x) = K(t, x-T_k\epsilon) + [K(t, x) - K(t, x-T_k\epsilon)] - (\epsilon/d)[T(K(t-\ell\epsilon, x+d)) - T(K(t-\ell\epsilon, x))]. \tag{14}$$

This is useful because a second order power series expansion of the second and third terms in this expression about point $(t, x-T_k\epsilon)$ yields an estimate of the error in (13) in terms of known quantities.

The expansion of the second term is:

$$[K(t, x) - K(t, x-T_k\epsilon)] \approx (T_k\epsilon)K_x + \tfrac{1}{2}\,(T_k\epsilon)^2K_{xx}\,,$$

where a double subscript denotes a second derivative. Likewise, the expansion of the third term can be reduced to:

$$-(\epsilon/d)[T(K(t-\ell\epsilon, x+d)) - T(K(t-\ell\epsilon, x))] \approx$$
$$-(\epsilon/d)[\ (dT_kK_x) \ + \ \tfrac{1}{2}(d^2 + 2dT_k\epsilon)(T_{kk}K_x^2 + T_kK_{xx}) \ - (d\ell\epsilon)(T_{kk}K_xK_t + T_kK_{xt})\ ],$$

and the sum of these two expressions can be further simplified. The combined result is:

$$-\tfrac{1}{2}d^2K_{xx}[(T_k\epsilon/d)^2 + (T_k\epsilon/d)] - \tfrac{1}{2}(T_{kk}K_x^2)(d\epsilon)[1 + 2(T_k\epsilon/d)] \ - (\ell\epsilon^2)(T_{kk}K_xK_t + T_kK_{xt}) \ ,$$

which allows us to rewrite (14) as follows:

$$K(t+\epsilon, x) \ \approx \ K(t, x-T_k\epsilon) \ - \ \tfrac{1}{2}d^2K_{xx}[(T_k\epsilon/d)^2 + (T_k\epsilon/d)]$$
$$- \ \tfrac{1}{2}(T_{kk}K_x^2)(d\epsilon)[1 + 2(T_k\epsilon/d)] \ - \ (\ell\epsilon^2)(T_{kk}K_xK_t + T_kK_{xt}). \qquad (15)$$

The first three terms of this expression coincide with (9) in Daganzo (1993a). The last term is the contribution to the error caused by the lag. This term becomes more meaningful if the time-derivatives K_t and K_{xt} are eliminated from the solution. This can be done if one notes from (3) that $k_t = - T_kk_x$, and that the x-derivative of this expression (keeping time constant) is: $k_{tx} = - T_{kk}k_x^2 - T_kk_{xx}$. If we use these relationships in the last term of (15) and use p as an abbreviation for $|T_k\epsilon/d|$, then we obtain the following expression for the error committed in time ϵ (when the system is congested):

$$\Theta \approx \ d^2K_{xx}p^2[\tfrac{1}{2}(1/p-1) - \ell] + T_{kk}K_x^2d\epsilon[\ -\tfrac{1}{2} + p(1+2\ell)]. \qquad (16)$$

This is the generalization of (10) in Daganzo (1993a).

When the system is uncongested, with T(k) = S(k), the LCT recipe does not use a lag. Therefore, the original derivation applies. The result is again (16), but with $\ell = 0$.

Note from (15) that the last three terms of that expression, i.e., what we have called Θ , represent the change in K(t, x) along the characteristic in time ϵ. Therefore, the ratio Θ/ϵ is the directional time-derivative of K(t, x) when $\epsilon \to 0$. Thus, in the case of a constant wave speed (i.e., linear T(k)) where the second term of (16) disappears because $T_{kk} = 0$, the value of K as seen by an observer moving with the wave satisfies the diffusion equation if ϵ is small. The solution of the diffusion equation is stable only if the diffusion coefficient is non-negative ; i.e., if the bracketed quantity in the first term (16) is non-negative. Thus, one should choose an ℓ that satisfies this condition for the largest possible p. This is the rationale for condition (11). Section 3.5, below, looks at the stability issue in a different way.

We have just seen that the second term of (16) vanishes if $T_{kk} = 0$. Note as well that if (12) is used to choose ℓ, then the first term will also vanish whenever the prevailing (backward) wave speed is at its maximum value. Since (16) also holds with $\ell = 0$ when the highway is uncongested, the first term also vanishes where the wave velocity is at its maximum value in the forward direction (i.e., when p = 1). Since the term also vanishes if p = 0, we see that the LCT model must be second order accurate when the T(k) relation is trapezoidal or triangular, provided that the lag is chosen with (12).

We also see from (16) that the (first order) errors arising from the first term of (16) should be proportional to the difference between the lag one would like to use for the given wave speed, which is $\frac{1}{2}(1/p - 1)$, and the actual lag. This difference is minimized with rule (12), and this is particularly important when T(k) is piecewise linear.

3.4 Variable meshes

The LCT method can be applied to highways and networks that have been discretized with cells of different lengths. In this more general case the LCT lag should be cell-dependent so as to ensure that the density is always read from the earliest possible time without violating the stability condition. That is, the lag for cell j , ℓ_j , should satisfy as tightly as possibly the inequality:

$$\epsilon \leq d_j / [|R_k|_{max} (2\ell_j + 1)], \tag{17}$$

where d_j is the cell length, instead of inequality (11).

To preserve the good properties of the LCT method, one should also introduce a forward lag, f_j , which should satisfy:

$$\epsilon \leq d_j / [S_{k,\, max} (2\mathsf{f}_j + 1)], \tag{18}$$

instead of (8). The forward lag can forestall the deterioration of accuracy where large cells are being used; especially if f_j is chosen so that (18) is as close to an equality as possible. The logic for this choice is the same as that in Sec. 3.3, and the outcome is also similar; e.g., in that the resulting method is still second order accurate in the case of a triangular T(k) relation.

The LCT rule with a variable discretization is then:

$$K(t+\epsilon, x_j) = K(t, x_j) - (\epsilon/d_j)[\ Q(t+\epsilon/2, x_j+d_j/2) - Q(t+\epsilon/2, x_j-d_j/2)\ ] \tag{19}$$

with

$$Q(t+\epsilon/2, x_j+d_j/2) = \min\{\ S(K(t-\mathsf{f}_j\epsilon, x_j))\ ,\ R(K(t-\ell_{j+1}\epsilon, x_{j+1})\}\ . \tag{20}$$

3.5. Stability and relationship to Godunov’s method

Godunov’s procedure identifies the stable solution because, as we have seen, its flows are always derived from the stable solution of a Riemann problem. Likewise, it will be shown here that the flows of the LCT method (20) are based on the *stable* solution of a modified Riemann problem, and therefore that the LCT solution should too approximate the stable solution.

Let us consider a modified Riemann problem (MRP) in which constant upstream and downstream densities have been defined on a V-shaped boundary, such as the dark line in Fig. 5. For an MRP problem to be well-posed, waves from both legs of the "V" should point into the solution space. This will happen if the (t, x)-slopes, s^u and s^d , of these legs satisfy $s^u > S_{k, max}$ and $s^d < -|R_k|_{max}$; i.e., if the V-shaped boundary is inside the shaded wedges shown in the figure.

Consideration reveals that the stable solution of the MRP for t > 0 is independent of the slopes of the "V" and that, as a result, said solution is also the stable solution of the conventional Riemann problem with the same initial densities. In other words, the stable flows arising at the discontinuity are the same for the conventional and modified Riemann problems.

Since (20) has the same form as (7), i.e., it is the minimum of a sending and a receiving value, it expresses the stable flow of a Riemann problem with $k^u = K(t-f_j\epsilon,\ x_j)$ and $k^d = K(t-\ell_{j+1}\epsilon,\ x_{j+1})$. As we have just shown, this is also the solution of a well-posed MRP with the same initial densities. In particular, it is the stable flow for the MRP in which the "V" passes through the lattice points at which k^u and k^d have been evaluated (points "A" and "B" in Fig. 5). This MRP will be well-posed if the "V"passing through the lattice points is inside the shaded wedges; i.e., if (17) and (18) are satisfied.

Thus, when (17) and (18) are satisfied the LCT method is nothing but a recursive solution of well-posed MRP's, just like the Godunov/CT method involves the recursive solution of ordinary Riemann problems. Insofar as the stable solution is always used in both procedures, we can conclude that the LCT method should share the good stability properties of the conventional CT method. The advantage of the former is that it is based on "older" data, which should be less corrupted by numerical errors.[7]

The following section presents some examples that illustrate both the accuracy and stability properties of the LCT method.

4. Examples

Let us start by examining the accuracy of the LCT model with both smooth and discontinuous initial conditions.

Tables 1 and 2 present 17 iterations of the conventional and lagged cell transmission models for a triangular flow-density relation of the form:

$$q = \min\{k, (180-k)/5\}, \qquad (21)$$

[7]The accuracy formulae of Sec. 3.3 confirm that the LCT method is most accurate when f_j and ℓ_{j+1} are chosen to be as large as possible, i.e., when the "V" forms as acute an angle as possible.

where k is in veh/mile and q in veh/min. It is assumed that the initial density profile is quadratic and in the congested range $k \in [30, 180]$; more specifically, that $k(0,x) = 50 + ½x^2$ and $x \approx 10 \pm 5$. Because the (congested) wave velocity is constant (i.e., $R_k = -0.2$) the exact solution of the problem in this range of x for small t is: $k(t, x) = 50 + ½(x+ t/5)^2$. That is, in the exact solution the density at mile x-1 must equal the density that prevailed at mile x five minutes earlier.

Table 1 presents the results of the ordinary CT model when one uses $\epsilon = 1$ and $d = 1$. In the exact solution the numbers in boldface would be equal, so that the observed discrepancy is the CT error. The discrepancies observed in the table are consistent with what would be expected from (16) with $\ell = 0$, and from the more detailed analysis in Daganzo (1993a).

If one uses the LCT model with $\epsilon = 1$, $d = 1$ and $\ell = 2$, i.e., the value recommended by (12), then Table 2 is obtained. In this case the LCT model reproduces the exact results, as one would expect from (16) and the analysis leading to it.[8]

Of course, the performance of the LCT procedure deteriorates in less favorable cases, e.g., with non-quadratic density profiles, non-linear T(k) functions, and non-ideal lags.

This is illustrated by Fig. 6, which contains the initial and final density profiles (at t = 25 min) for a Riemann initial value problem where (21) holds and where the initial density changes suddenly from k = 50 to k = 100 at x = 20 mile. The thin lines are the CT and LCT results obtained with $\epsilon = 1$ min and d = 1 mile. Note the lesser spread of the LCT result, and that the LCT model does not transition monotonically from one density value to the other.[9] The relative accuracy of the two models can be evaluated better with the cumulative curves of vehicle count; see Fig. 7. Whereas in the CT model the maximum error in vehicle position is on the order of 2/3 miles (which is not surprising since d = 1 mile), with the LCT the largest error is less than 1/5 mile.

In order to illustrate the stability of the method for non-concave T(k) relations, Figs. 8 and 9 depict the LCT solution of the lead vehicle problem in Fig. 2c using cells with d = 100 m and time steps $\epsilon = 2$ secs. This is efficient because with this arrangement (8) is satisfied as an equality -- note from Fig. 2a that in our case $|T_k|_{max} = v_f = 50$ m/s. Since $|R_k|_{max} = 350/13$ m/s, the optimum lag according to (12) should be $\ell = 3/7$. Because this is not an integer, R(k) was evaluated for a k that was an interpolation of the densities obtained with $\ell = 0$ and $\ell = 1$. The numerical results should then still be second order accurate for densities less than or equal to that of state "E" in Fig. 2a, and less accurate for more congested states.

The density profiles of Fig. 8 confirm this. Note how the curves have sharper steps below the line K = 0.5 than near the top. (In the exact solution these curves would be perfect step functions.) Note as well the good agreement between this figure and 2c; in particular, the development of intermediate state "E", with $K \approx 0.4$, after t = 120 secs.

---

[8]Note that, for this to be the case, $\ell +1$ time slices of internally consistent initial data had to be specified.

[9] This undesirable feature of the LCT model is typical of second order approximations (see, e.g., LeVeque, 1992). As a result, the LCT model may produce densities slightly greater than the theoretical maximum from time to time. Therefore, the receiving function R(k) should be defined for $0 < k < \infty$, in an implementation.

Figure 9 displays the N-curves (of vehicle number) at five locations in ½ Km increments upstream of the stoppage. They also agree qualitatively with the exact solution of the problem, which in this case is piecewise linear. Clearly, the curved arcs in the figure, which correspond to episodes of very congested traffic, have some numerical error. However, the straight portions of the curves match the exact solution precisely, and therefore it is easy to ascertain from the figure the magnitude of the numerical errors in the curved sections. This error does not exceed 5 vehicles in any of the curves.

5. CONCLUSION

The LCT procedure is also well suited for modeling intersections and inhomogeneous highways, since the only change needed in the existing procedures is reading the traffic density for the downstream conditions with a time lag. This modification is so minor that it can also be applied to highways with special lanes and their junctions; e.g. by modifying the procedure described in Daganzo *et al.* (1995).

It should also be said that lags impose additional memory storage requirements on an LCT simulation, since cell densities must be stored for the past $1+\ell_j$ time slices. For multi-destination networks, however, most of the storage is consumed by the cell content proportions (by destination and entry time), which are only used as arguments as part of the "sending" functions. Thus, in an LCT implementation the bulk of the information would only have to be kept for $1+\mathbf{f}_j$ time slices.

REFERENCES

Bui, D.D., P. Nelson and S. L. Narasimhan (1992) Computational realizations of the entropy condition in modeling congested traffic flow. FHWA Report TX-92/1232-7.

Cassidy, M. (1998), Bivariate relations in highway traffic. *Trans. Res.* **32B**(1), 49-59.

Daganzo, C.F. (1993) The cell-transmission model: A dynamic representation of highway traffic consistent with the hydrodynamic theory. Institute of Transportation Studies, Research Report, UCB-ITS-RR-93-7, Univ. of California, Berkeley, CA. Short version in *Trans. Res.*, 28B(4), 269-287.

Daganzo, C.F. (1993a) A finite difference approximation for the kinematic wave model. Institute of Transportation Studies, Research Report, UCB-ITS-RR-93-11, Univ. of California, Berkeley, CA. Short version in *Trans. Res.* **29B**(4) 261-276.

Daganzo, C.F. (1994) The cell-transmission model. Part II: Network traffic. PATH working paper UCB-ITS-PWP-94-12, Univ. of California, Berkeley, CA. Short version in *Trans. Res.*, **29B**(2), 79-94.

Daganzo, C.F. (1995) A continuum theory of traffic dynamics for freeways with special lanes. PATH Technical Note UCB-ITS-PTN-95-08, Univ. of California, Berkeley, CA. Short version in *Trans Res.* **31B** (2), 83-102.

Daganzo, C.F. (1997) An enhanced cell-transmission rule for traffic simulation. Institute of Transportation Studies Research UCB-ITS-RR-97-06, Univ. of California, Berkeley, CA.

Daganzo, C.F., Lin, W.H. and del Castillo, J.M. (1995) A simple physical principle for the simulation of freeways with special lanes and priority vehicles. PATH Technical Note UCB-ITS-PTN-95-09, Univ. of California, Berkeley, CA. Short version in *Trans. Res.* **31B** (2), 105-125.

Godunov, S.K. (1961) Bounds on the discrepancy of approximate solutions constructed for the equations of gas dynamics. *J. Com. Math. and Math. Phys.* **1**, 623-637.

Herman, R., E.W. Montroll, R.B. Potts, and R.W. Rothery (1959), "Traffic dynamics: Analysis of stability in car following", *Opns. Res.* **7**, 86-106.

Lax, P.D. (1973) *Hyperbolic systems of conservation laws and the mathematical theory of shockwaves*. Regional Conf. Series in Applied Mathematics. SIAM, Philadelphia, PA.

Lebacque, J.P. (1993) Les modèles macroscopiques de trafic. *Annales de Ponts*, (3rd trim) **67**, 28-45.

LeVeque, R.J. (1992) *Numerical methods for conservation laws,* (2nd edition), Birkhauser-Verlag, Boston, MA.

Lighthill, M.J. and G.B. Whitham (1955) On kinematic waves. I flow movement in long rives. II A theory of traffic flow on long crowded roads. *Proc. Roy. Soc. A*, **229**, 281-345.

Luke, J.C. (1972) Mathematical models for landform evolution. *J.Geophys. Res.*, **77**, 2460-2464.

Newell, G.F. (1961) Non-linear effects in the dynamics of car-following. *Opns. Res.* **9**(2), pp. 209-229.

Newell, G.F. (1993) A simplified theory of kinematic waves in highway traffic, I general theory, II queuing at freeway bottlenecks, III multi-destination flows. *Trans. Res.*, **27B**, 281-313.

Richards P.I. (1956) Shockwaves on the highway. *Opns. Res.*, **4**, 42-51.

Windover, J. and Cassidy, M.J. (1997) Private communication.

Table 1. Estimated densities at different positions with the cell-transmission model. Row 3 is the position (x) in Km. Rows 5 and 6 are the maximum flow and the jam density at the given position. Rows 9 to 11 are the initial data, $k = 50 + ½(x + t/5)^2$, where t = 0 for row 9, t = 1 for row 10 and t = 2 for row 11.

3	6	7	8	9	10	11
4						
5	30	30	30	30	30	30
6	180	180	180	180	180	180
7						
8						
9	68	74.5	82	90.5	100	110.5
10	69.22	75.92	83.62	92.32	102.02	112.72
11	70.48	77.38	85.28	94.18	**104.08**	114.98
12	71.86	78.96	87.06	96.16	106.26	117.36
13	73.28	80.58	88.88	98.18	108.48	119.78
14	74.74	82.24	90.74	100.24	110.74	122.24
15	76.24	83.94	92.64	102.34	113.04	124.74
16	77.78	85.68	94.58	**104.48**	115.38	127.279
17	79.36	87.46	96.56	106.66	117.76	129.852
18	80.98	89.28	98.58	108.88	120.178	132.453
19	82.64	91.14	100.64	111.14	122.633	135.071
20	84.34	93.04	102.74	113.438	125.121	137.694
21	86.08	94.98	**104.88**	115.775	127.635	140.308
22	87.86	96.9599	107.059	118.147	130.17	142.897
23	89.68	98.9796	109.276	120.551	132.715	145.445
24	91.5399	101.039	111.531	122.984	135.261	147.936
25	93.4397	103.137	113.822	125.44	137.796	150.355
26	95.3793	**105.274**	116.145	127.911	140.308	152.691
27	97.3583	107.449	118.499	130.39	142.785	154.931
28	99.3763	109.659	120.877	132.869	145.214	157.066
29	101.433	111.902	123.275	135.338	147.584	159.09

Table 2. Estimated densities at different positions with the lagged cell-transmission model. Row 3 is the position (x) in Km. Rows 5 and 6 are the maximum flow and the jam density at the given position. Rows 9 to 11 are the initial data, $k = 50 + ½(x + t/5)^2$, where t = 0 for row 9, t = 1 for row 10 and t = 2 for row 11.

3	6	7	8	9	10	11
4						
5	30	30	30	30	30	30
6	180	180	180	180	180	180
7						
8						
9	68	74.5	82	90.5	100	110.5
10	69.22	75.92	83.62	92.32	102.02	112.72
11	70.48	77.38	85.28	94.18	**104.08**	114.98
12	71.78	78.88	86.98	96.08	106.18	117.28
13	73.12	80.42	88.72	98.02	108.32	119.62
14	74.5	82	90.5	100	110.5	122
15	75.92	83.62	92.32	102.02	112.72	124.42
16	77.38	85.28	94.18	**104.08**	114.98	126.88
17	78.88	86.98	96.08	106.18	117.28	129.38
18	80.42	88.72	98.02	108.32	119.62	131.92
19	82	90.5	100	110.5	122	134.5
20	83.62	92.32	102.02	112.72	124.42	137.12
21	85.28	94.18	**104.08**	114.98	126.88	139.78
22	86.98	96.08	106.18	117.28	129.38	142.48
23	88.72	98.02	108.32	119.62	131.92	145.22
24	90.5	100	110.5	122	134.5	148
25	92.32	102.02	112.72	124.42	137.12	150.82
26	94.18	**104.08**	114.98	126.88	139.78	153.677
27	96.08	106.18	117.28	129.38	142.48	156.565
28	98.02	108.32	119.62	131.92	145.22	159.47
29	100	110.5	122	134.5	147.999	162.369

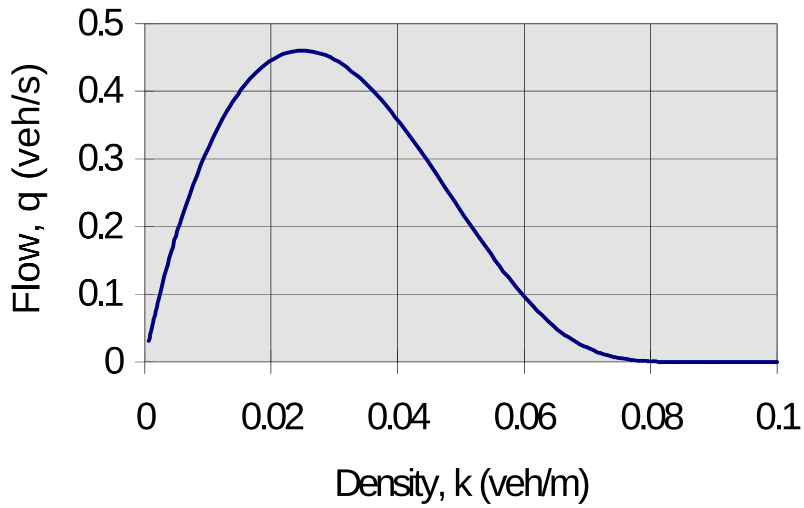

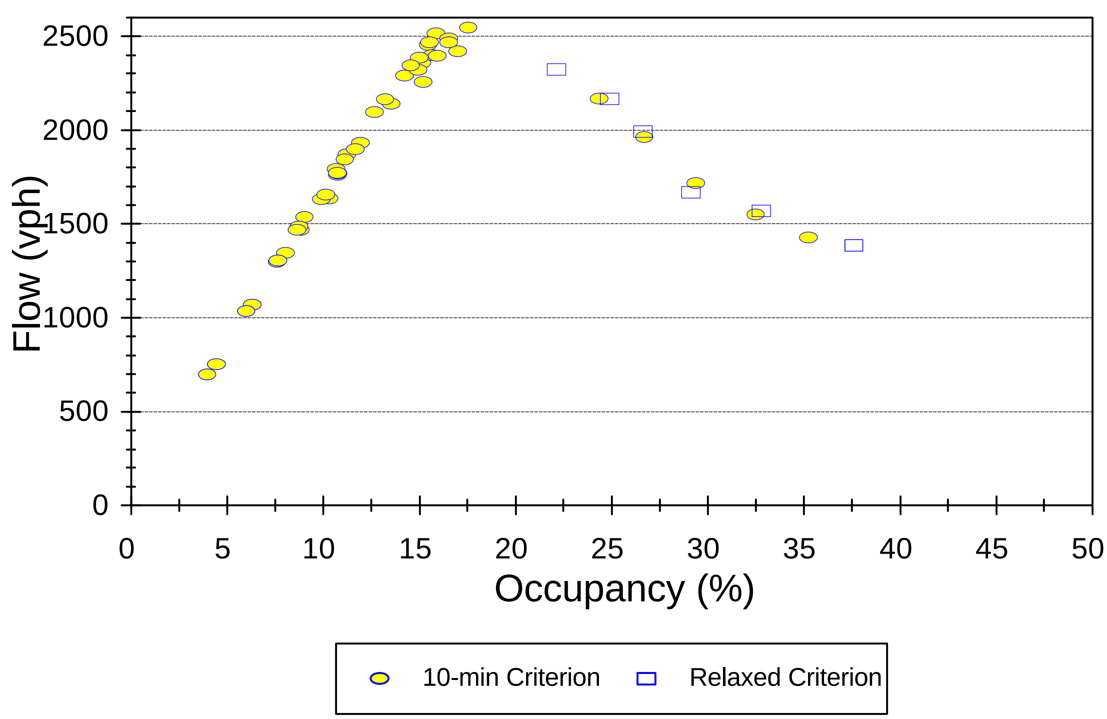

Figure 1. Stationary relations between traffic variables. Top: hypothetical non-concave relation between flow and density. Bottom: actual form of a steady-state relationship between flow and occupancy (source: Cassidy, 1996).

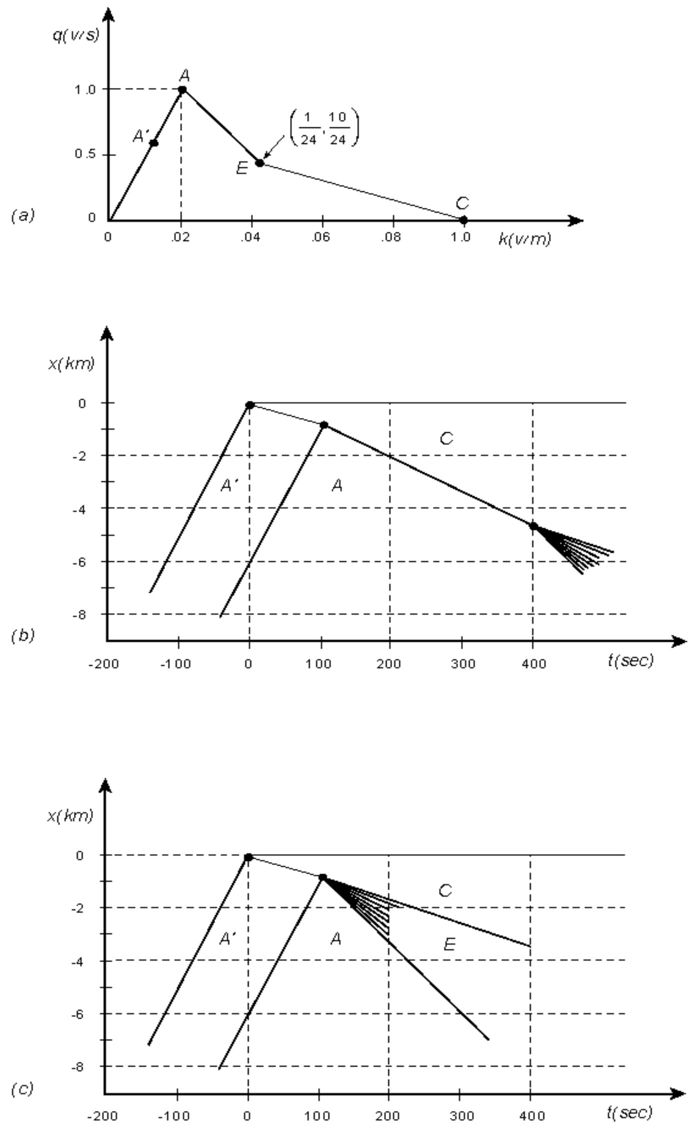

Figure 2. Solutions of a lead-vehicle problem with kinematic wave theory: (a) T(k) relation; (b) a mathematically valid but physically unacceptable solution; and (c) the stable solution.

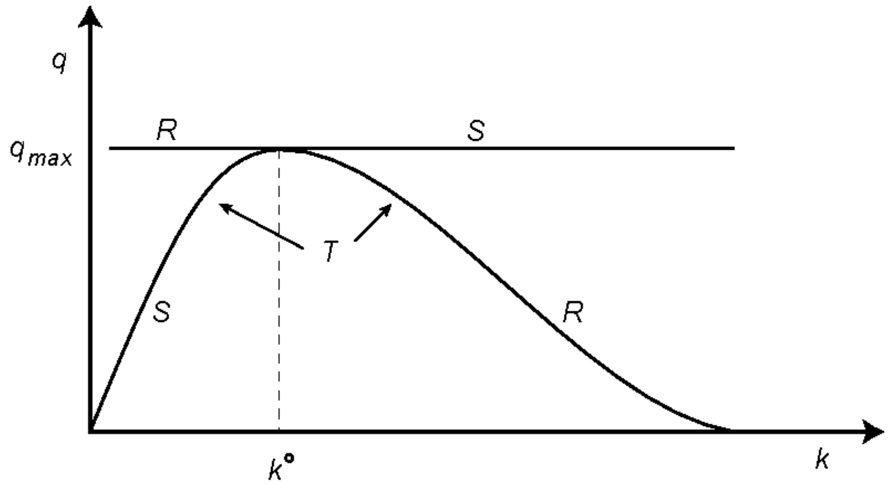

Figure 3. Sending and receiving functions of the cell-transmission model.

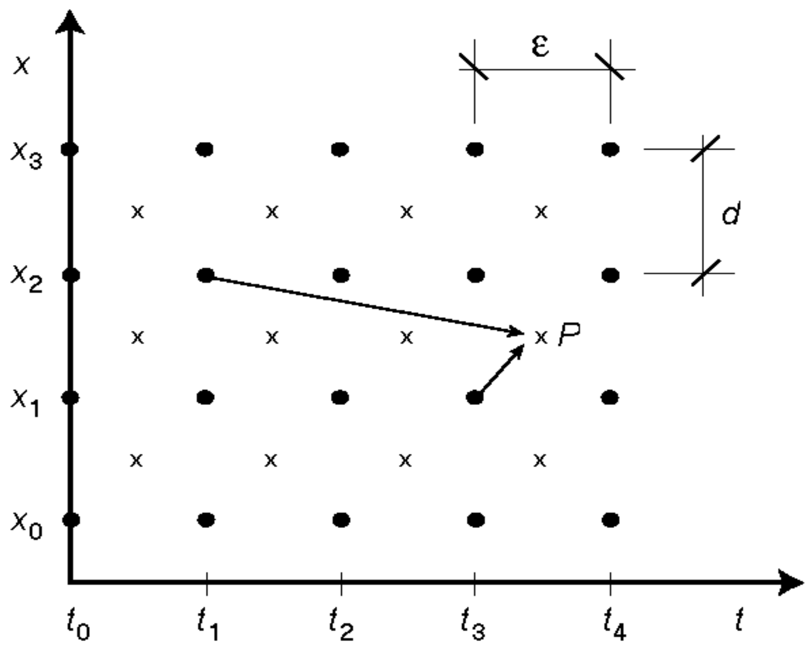

Figure 4. Lattice and stencil for the lagged cell-transmission model. Dots are lattice points; crosses are points where the average flows are evaluated.

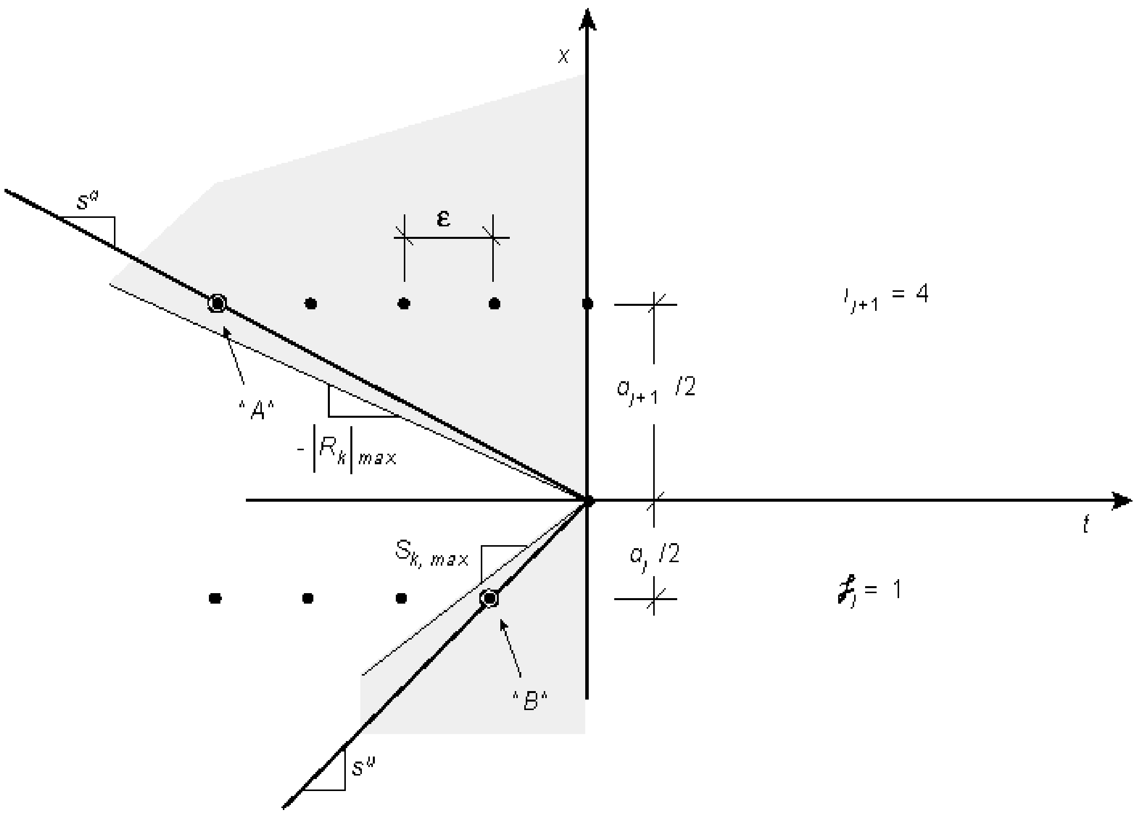

Figure 5. The modified Riemann problem at the core of the LCT.

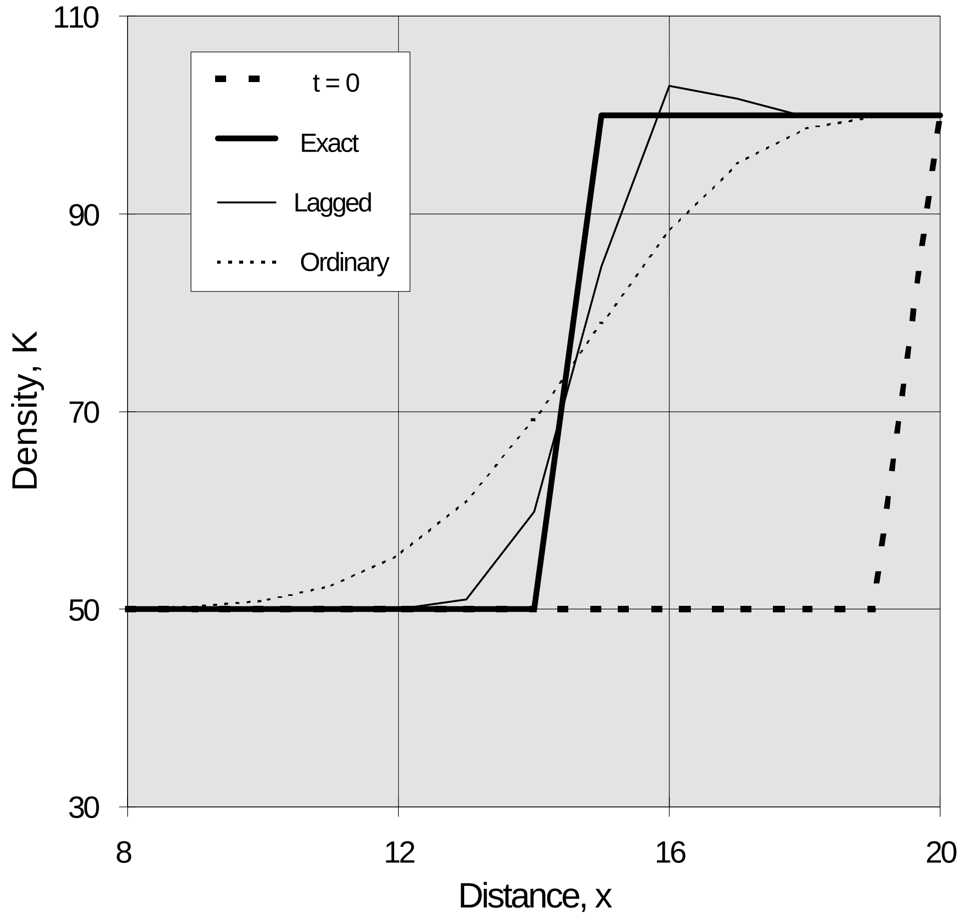

Figure 6. Evolution of a discontinuous traffic disturbance as predicted by the CT and LCT models for the case of a triangular T(k) curve with p = 0.2: density profile comparison..

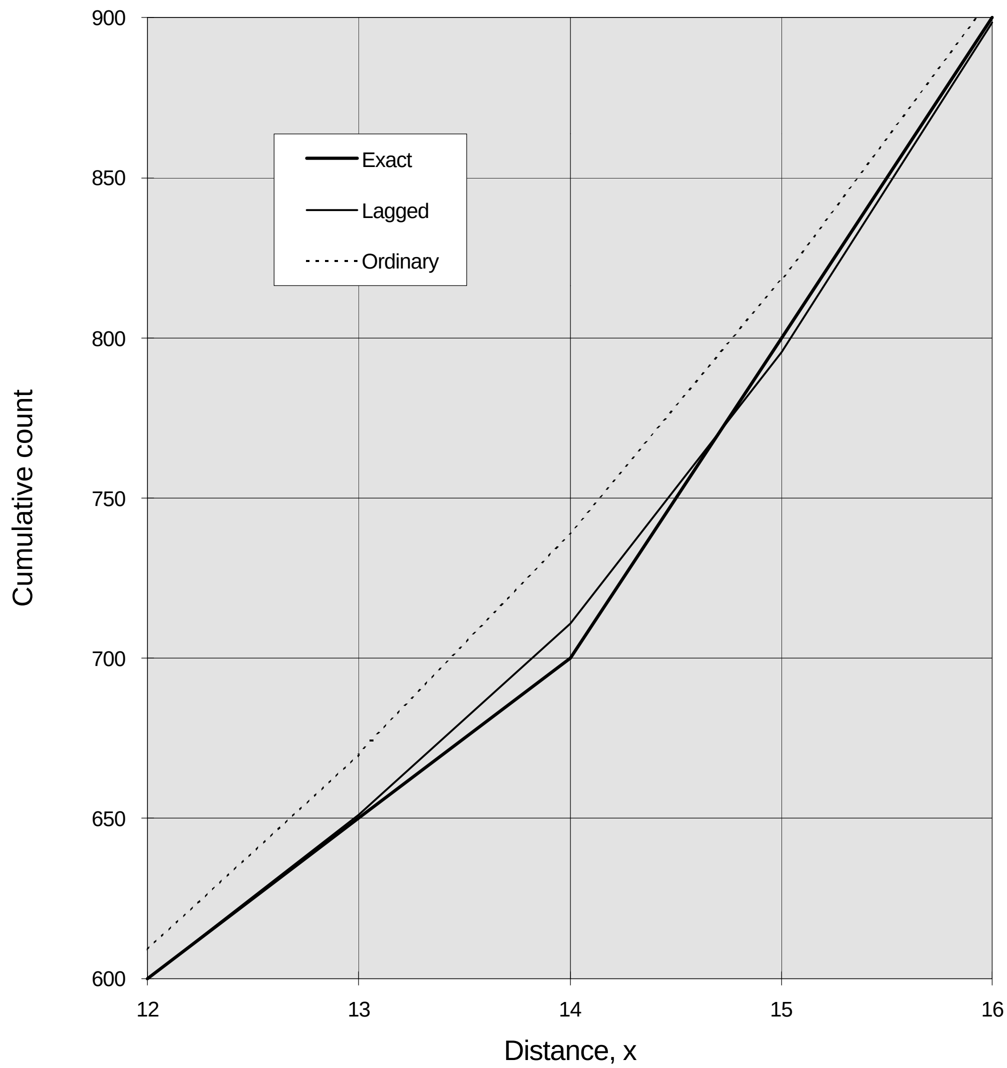

Figure 7. Evolution of a discontinuous traffic disturbance as predicted by the CT and LCT models for the case of a triangular T(k) curve with p = 0.2: cumulative vehicle count comparison.

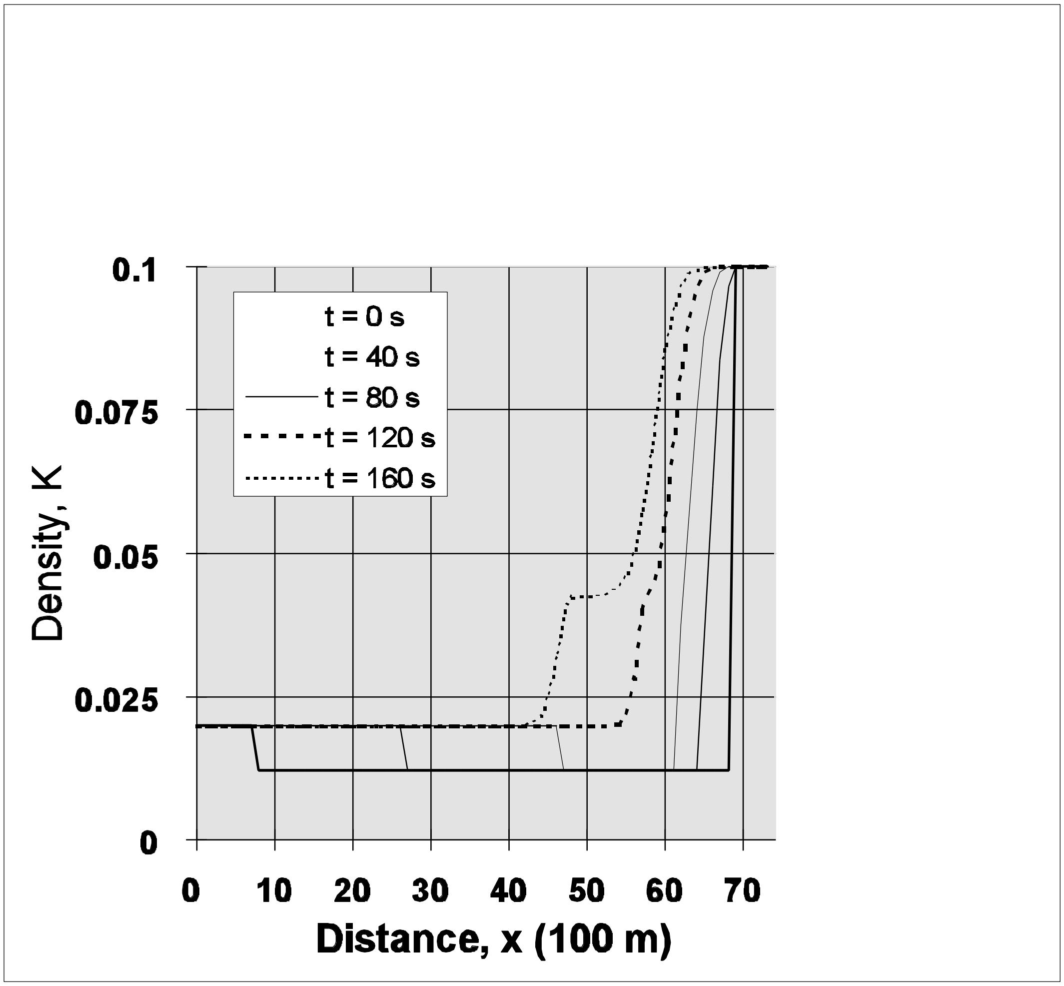

Figure 8. Density profiles for the lead vehicle problem of Fig. 2.

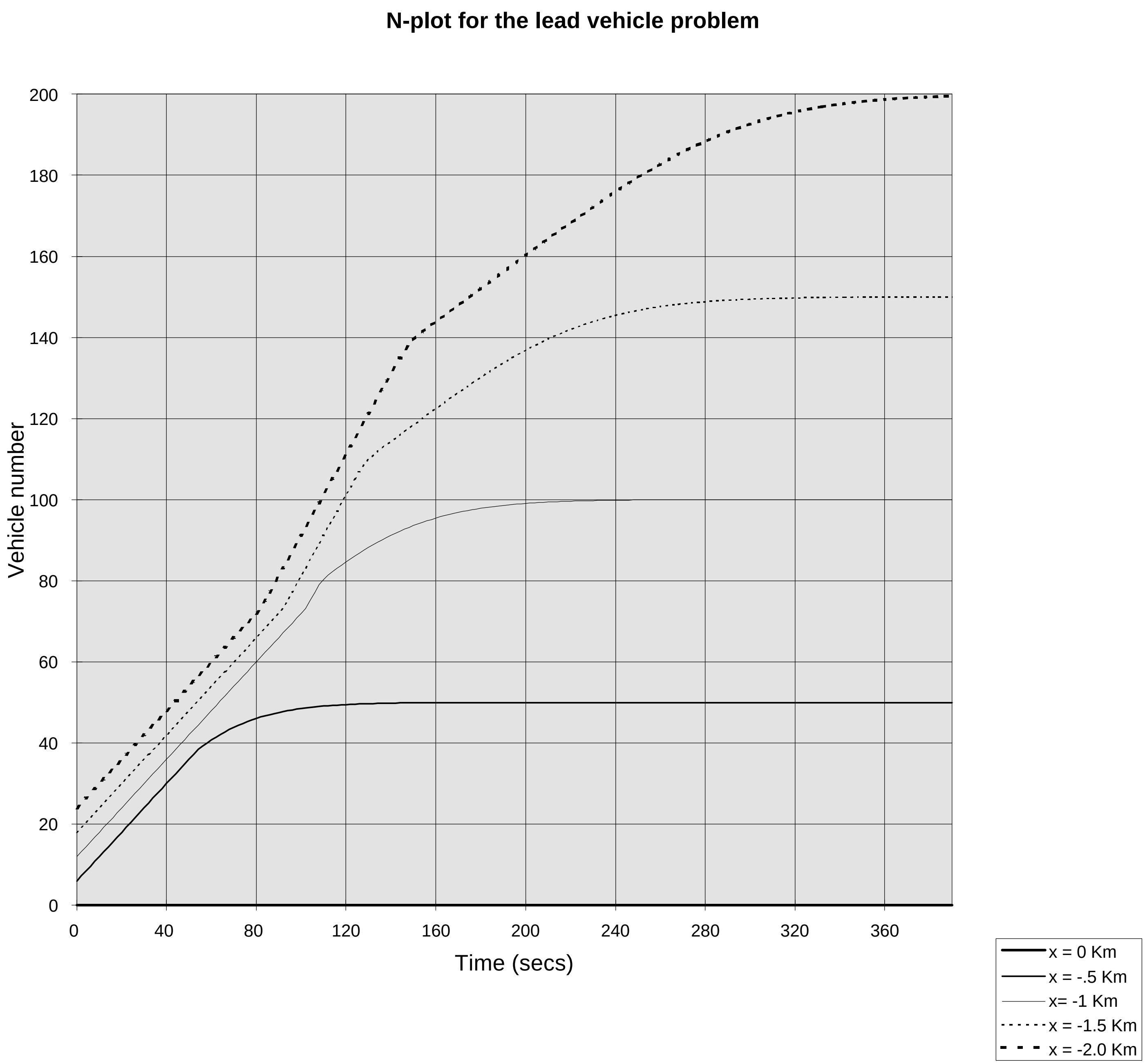

Figure 9. N-curves for the lead vehicle problem of Fig. 2.